Research Article

Journal of Environmental Nanotechnology

Analysis on Microstructural Properties, Morphology and Electrochemical Performance Kinetics of Monoclinic CuO Nanoparticles

N. Nejanthan[1], J. Varuna[2], J. Manikandan[1], M. Elango[2], S. Chandra[1] and J. Raffiea Baseri[1*]

[1]Department of Chemistry, PSG College of Arts and Science, Coimbatore, TN, India

[2]Department of Physics, PSG College of Arts and Science, Coimbatore, TN, India

Received: 25.01.2025 Accepted: 18.03.2025 Published: 30.03.2025

*raffiea2010@gmail.com

ABSTRACT

Copper oxide (CuO) nanoparticles were thoroughly analyzed to evaluate their structural, morphological, optical and electrochemical properties. X-ray diffraction (XRD) study confirmed the monoclinic phase and high crystallinity of the prepared nanoparticles, with crystallite sizes ranging between 16 - 21 nm. High-resolution scanning electron microscopy (HRSEM) revealed a mixture of porous, rod-like, and sheet-like morphologies, while transmission electron microscopy (TEM) demonstrated the presence of nanoscale particles of dimensions 10 - 20 nm and chain-like aggregations. Raman spectroscopy validated the monoclinic structure, with characteristic A_g and B_g vibrational modes. UV-Vis spectroscopic analysis highlighted a quantum confinement effect, with a blue-shifted absorption peak at 306 nm and a bandgap of approximately 3.8 eV. Electrochemical investigations using Nyquist plots and cyclic voltammetry (CV) revealed excellent pseudo capacitive behavior, with low charge transfer resistance (R_{ct}) and stable redox processes. The electrochemical impedance spectroscopy (EIS) plot indicated effective ion diffusion and good conductivity, making CuO nanoparticles as promising candidates for energy storage applications such as super capacitors and batteries. The rate constant for the irreversible adsorption-controlled electrochemical process was calculated using Laviron plot.

Keywords: CuO nanoparticles; GCD analysis; Irreversible electrode; Laviron plot.

1. INTRODUCTION

Nanotechnology is emerging as a transformative technology in areas such as medicine, cosmetics, environmental health, energy science and space industries, offering innovative solutions to various challenges (Bezza *et al*. 2020). However, the introduction of novel nanoparticles possess potential risks, as they may interact with the immune system and trigger inflammatory responses (Liu *et al.* 2022). Nanoparticles can be synthesized through various methods, including chemical, physical, and biological approaches, each offering unique advantages depending on the intended application (Crisan *et al.* 2022). Among metal nanoparticles, copper oxide nanoparticles (CuO NPs) have attracted considerable attention due to their non-toxic nature, cost-effectiveness, natural abundance and simple fabrication techniques (Mohamed *et al.* 2021). These nanoparticles exhibit remarkable properties such as a large surface area, good electrochemical activity, stability in solutions and appropriate redox potential, making them highly versatile for numerous applications.

CuO nanoparticles have been extensively utilized in nano science for a wide range of applications. Their biocidal properties make them suitable as antimicrobial agents, while their ability to act as drug delivery vehicles enhances therapeutic efficacy (Grigore *et al.* 2016). Additionally, CuO NPs are employed in antifouling coatings, sensors and biosensors due to their excellent chemical and physical stability (Sarfraz *et al.* 2020). The potential of CuO nanoparticles for use in photovoltaic cells and other energy applications further underscores their importance in advancing sustainable technologies.

2. MATERIALS AND METHODS

2.1 Materials

All chemical of high purity were purchased from Merck (India) and were used as received. The precursor materials used are copper chloride ($CuCl_2$), sodium hydroxide (NaOH), acetone (C_3H_6O), ethanol (C_2H_5OH) and deionized water.

2.2 Preparation Protocol

About 25 mL of 0.1 M $CuCl_2$ was placed in a beaker and stirred using a magnetic stirrer. Then, 10 mL of 0.2 M NaOH was added drop wise and stirred for 4 hours. After that, Whatmann (no.40) filter paper was

used to filter the colloidal solution. The filtrate was collected in a silica crucible and dried in a muffle furnace for 4 hours at 400 ℃.

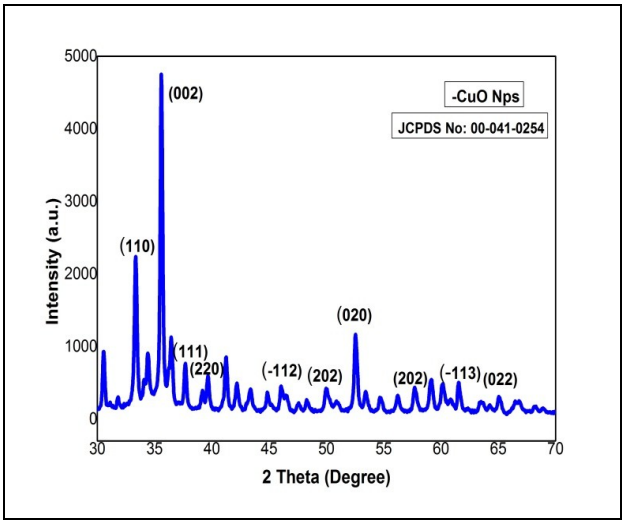


Fig. 1: XRD spectrograph of CuO nano particles

3. SAMPLE CHARACTERIZATION

The characterization techniques namely structural, morphological and optical investigations were made by XRD, HRSEM, HRTEM, Raman and UV-Visible spectroscopic methods. A three-electrode system was used to study the electrochemical activity of the materials using KOH as electrolyte.

3.1 X-ray Diffraction Analysis

The XRD pattern of CuO nanoparticles exhibits distinct diffraction peaks that confirms the monoclinic phase and crystalline structure of the material (Mobarak *et al*. 2022). Prominent peaks were observed at 2θ values of 35.55°, 35.57°, 38.41° and 38.73°, which correspond to the crystal planes (002), (111) and (200) respectively (Fig. 1). Additional peaks are assigned to crystal planes such as (110), (-112), (202), (020), (202), (113), (022), (311), (-113), (220) and (311) confirming the monoclinic CuO phase according to the JCPDS card number 00-041-0254. The sharpness and intensity of the diffraction peaks indicate the high degree of crystallinity in the synthesized nanoparticles, while the absence of any extraneous peaks demonstrates the phase purity of the material.

The crystallite size of CuO nanoparticles, calculated using the Scherrer equation, falls in the range 16 - 20 nm, confirming the nanoscale dimensions of the material (Table 1).

Peak broadening in the XRD pattern indicates lattice strain, which is a typical characteristic of nanomaterial that may arise from surface defects and the high surface-to-volume ratio of nanoparticles. These findings validate the structural integrity and purity of CuO nanoparticles, making them highly suitable for applications requiring high crystallinity, such as catalysis, energy storage and sensors. Furthermore, the monoclinic structure and nanoscale features of CuO nanoparticles contribute to its unique physical and chemical properties, which are crucial for enhancing its performance in practical applications. The absence of secondary phases or impurities further emphasizes the successful synthesis of phase-pure CuO nanoparticles.

Table 1: Microstructural properties of CuO NPs

Miller Plane	Crystallite size (nm)	Micro strain (ε)	Stacking fault	Dislocation density (dislocation/m^3)	Lattice parameter (Å)
(110)	20.25	0.0039	0.00181	0.0004881	a = 4.952
(002)	18.46	0.0035	0.00173	0.0004838	b = 3.854
(020)	15.93	0.0027	0.00139	0.0003337	c = 5.695

3.2 HRSEM and EDAX Analysis

The High-Resolution Scanning Electron Microscopy (HRSEM) analysis of CuO nanoparticles reveals a distinctive rod-like and sheet-like morphology, with particle dimensions ranging from ten to several hundred nanometers (Fig. 2).

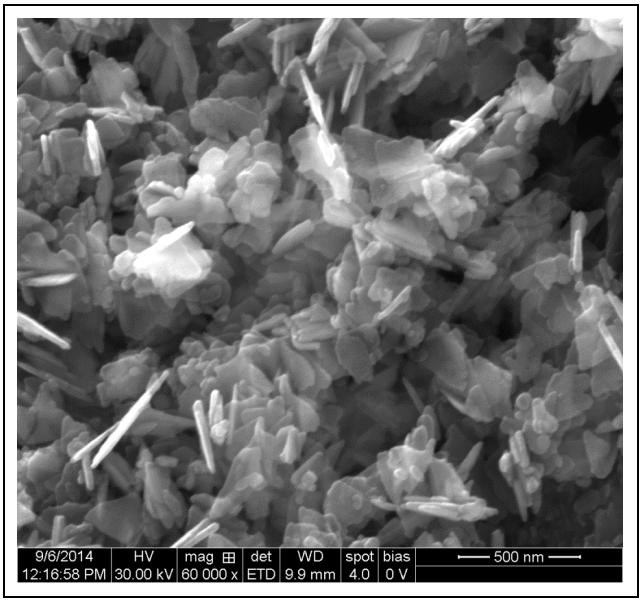


Fig. 2: HRSEM image of CuO nanoparticles

This anisotropic growth pattern during synthesis contributes to an increased surface area, enhancing the material's suitability for catalytic and energy storage applications. Similar morphological characteristics have been reported in the literature (Pal *et al.* 2014), highlighting the influence of synthesis conditions on the structural attributes of CuO nanostructures.

The observed aggregation of nanoparticles is likely due to Van der Waals forces or magnetic interactions, which can marginally reduce surface

accessibility. Despite this, the inherent high surface area of the rod-like and sheet-like structures remains advantageous for various applications. Porous architectures in CuO nanostructures have been synthesized using methods such as thermal oxidation, resulting in materials with enhanced surface areas and pore volumes, beneficial for applications requiring efficient ion transport and adsorption (Ahmed *et al.* 2023).

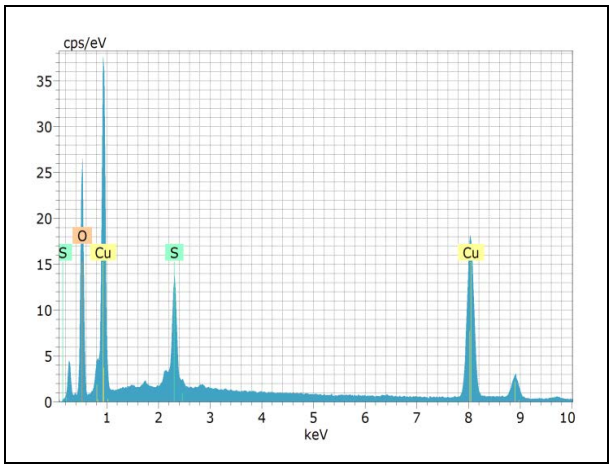


Fig. 3: EDAX spectrum of CuO nanoparticles

Energy-dispersive X-ray spectroscopy (EDX) analysis (Fig. 3) confirms the elemental composition of the synthesized CuO nanoparticles, indicating the presence of copper and oxygen. This compositional purity is crucial for the reliability and performance of CuO NPs in practical applications. The combination of HRSEM and EDX analyses provides a comprehensive understanding of the morphological and compositional properties of CuO nanostructures.

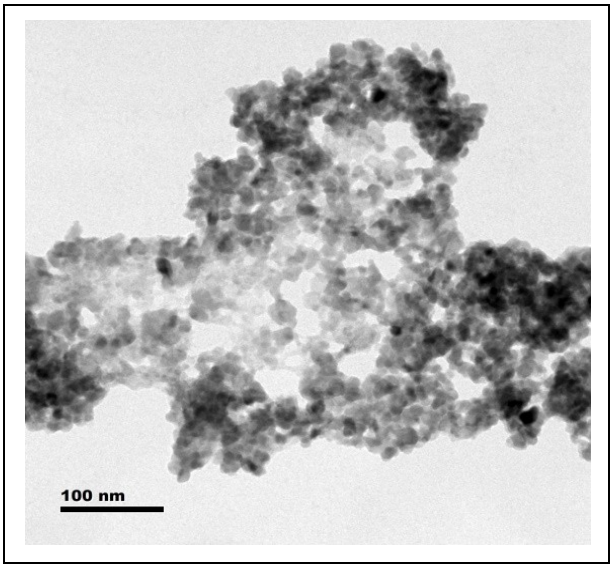


Fig. 4: HRTEM image of CuO nanoparticles

3.3 HRTEM Analysis

The high-resolution transmission electron microscopy (HRTEM) image of CuO nanoparticles reveals their aggregated nature, with individual particles measuring between 10 and 20 nm in diameter (Fig. 4). The observed spherical and slightly irregular particle shapes indicate controlled nucleation and growth processes during synthesis. The aggregation of these nanoparticles forms chain-like structures, which may impact their conductivity and ion transport properties. These nanoscale dimensions align with the crystallite sizes determined through XRD analysis, further validating the uniformity of the synthesized CuO nanoparticles.

The dark regions visible in the HRTEM image represent areas of high electron density, signifying well-crystallized nanoparticles. The absence of discernible lattice fringes in the image implies that higher magnification or resolution may be required to explicitly confirm crystallinity. Despite this, the well-defined structural features observed emphasize the superior nanoscale effects and structural uniformity of the material. Such characteristics are pivotal for various high-performance applications, including catalysis, energy storage, and sensing technologies.

These findings reinforce the potential of CuO nanoparticles as functional nanomaterials, leveraging their size-dependent properties and structural uniformity for advanced applications.

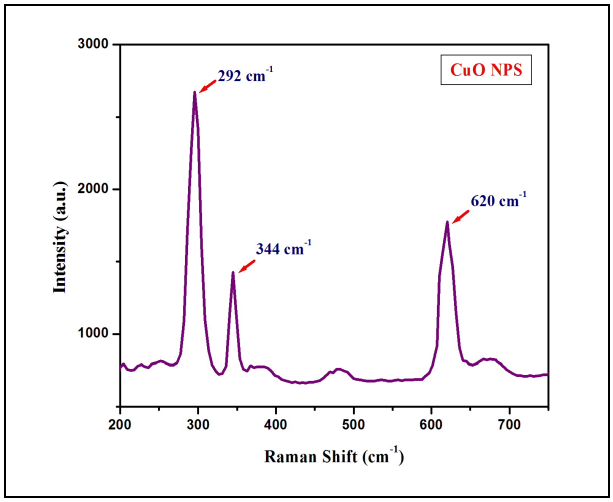


Fig. 5: Raman spectrum of CuO nanoparticles

3.4 Raman Analysis

Raman spectroscopy serves as a powerful tool for understanding the vibrational dynamics and defect structures of CuO nanoparticles. The findings align with prior studies that highlight the role of surface defects and

lattice distortions in tailoring the properties of nanomaterial (Tite *et al.* 2019).

The Raman spectrum shown in Fig. 5 exhibits distinct peaks that correspond to the vibrational modes of the monoclinic phase, confirming the structural integrity of the CuO. A prominent peak observed at approximately 292 cm^{-1} is assigned to the symmetric A_g mode, which corresponds to the Cu-O bond stretching vibrations. Additional peaks, including a signal around 344 cm^{-1} and 620 cm^{-1}, are attributed to the B_g modes, representing asymmetric vibrations in the lattice. These characteristic modes validate the presence of the monoclinic phase and confirm the structural purity of the synthesized CuO nanoparticles.

The broadening of the Raman peaks, particularly in comparison to bulk CuO, highlights the influence of quantum confinement effects and surface-related defects that are inherent in nanostructures. These broadened peaks also suggest a reduction in particle size, as quantum effects become more pronounced in nanoparticles.

3.5 UV-Vis Analysis

The UV-Vis spectrograph of CuO nanoparticles shown in Fig. 6 reveals a strong absorption peak at 306 nm, suggesting a significant blue shift compared to that of bulk CuO. This shift indicates a quantum confinement effect due to the reduced particle size (Rehman *et al.* 2011). The bandgap energy, estimated from the Tauc plot, was approximately 3.8 eV, demonstrating the nanoscale-induced modification of electronic properties.

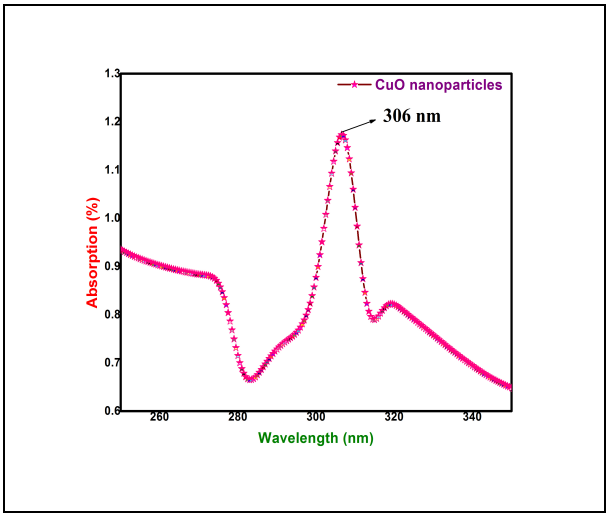


Fig. 6: UV Visible absorption spectrum of CuO nanoparticles

The strong interaction with UV light suggests the enhanced photo catalytic efficiency, making CuO nanoparticles suitable for environmental and energy-related technologies (Munawar *et al.* 2020).

3.6 FTIR Spectroscopic Analysis

The FTIR spectrum of CuO nanoparticles reveals distinct vibrational modes, providing critical information about the structural and chemical characteristics of the material (Atri *et al.* 2023). A broad band observed around 2972.31 cm^{-1} is attributed to the stretching vibrations, likely originating from adsorbed water molecules or surface hydroxyl groups (Fig 7). Such features are commonly associated with nanomaterials synthesized in aqueous media or those exposed to atmospheric moisture. These hydroxyl groups can influence surface chemistry and interaction properties, making them essential for understanding the nanoparticle's potential reactivity and stability in various applications (Andualem *et al.* 2020).

The mid-wavenumber region, particularly the peak at 1627.92 cm^{-1}, indicates the presence of surface-adsorbed water molecules. This feature is commonly observed in FTIR studies of metal oxide nanoparticles and underscores the role of surface hydration in affecting the materials catalytic and electrochemical performance (Kamnev *et al.* 2021). Presence of these vibrational modes confirms the expected chemical composition.

In the low-wavenumber region, the prominent peaks at 530.42 cm^{-1} and 636.51 cm^{-1} are characteristic of Cu-O stretching vibrations, a signature of monoclinic CuO. Additional peaks, such as those at 873.75cm^{-1} and 1006.84 cm^{-1}, may correspond to lattice vibrations or weak contributions from surface impurities. These confirm the successful synthesis of CuO nanoparticles (Alhalili, 2022).

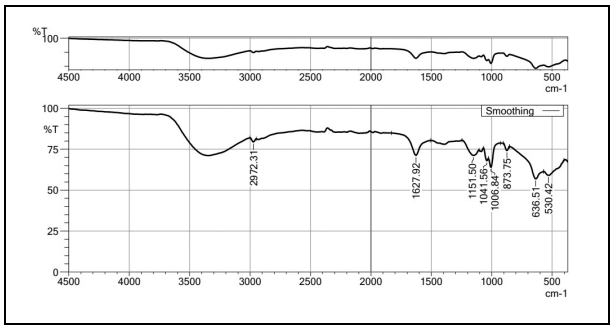


Fig. 7: FTIR spectrum of CuO nanoparticles

3.7 Nyquist Plot (GCD Analysis)

The Nyquist plot (Fig. 8) of CuO nanoparticles recorded at a current density of 5 mA provides valuable insights into their electrochemical behavior. The plot features a prominent semicircular arc in the high-frequency region, representing the charge transfer resistance (R_{ct}). The relatively large semicircle indicates higher R_{ct}, which reflects slower charge transfer kinetics at the electrode-electrolyte interface. This behavior

suggests moderate electronic conductivity under these conditions.

At lower frequencies, the Warburg tail is evident, signifying ion diffusion limitations in the CuO nanoparticles. The slope of the Warburg tail highlights moderate ion transport properties, which are critical for optimizing the material's performance in electrochemical applications (Kosmaca *et al*. 2023)

The findings from the Nyquist plot highlight the current-dependent electrochemical performance of CuO nanoparticles. The semicircular arc at high frequencies decreases significantly under these conditions, indicating enhanced charge transfer and reduced resistance. This improvement in conductivity is further supported by the reduced Warburg impedance observed at lower frequencies, which signifies better ion transport through the electrode material.

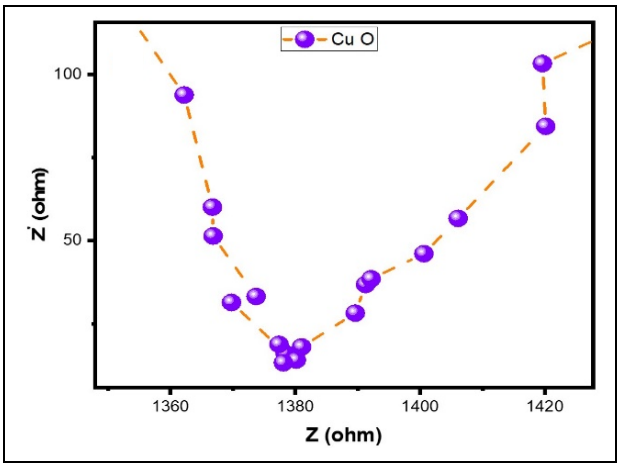


Fig. 8: GCD analysis of CuO nanoparticles at 5 mA

These properties make CuO nanoparticles highly promising for high-rate energy storage applications. Overall, the electrochemical impedance spectroscopy (EIS) analysis emphasizes the role of CuO nanoparticles as efficient electrode materials due to their low charge transfer resistance, improved ion diffusion, and superior current-carrying capabilities (Aziz *et al.* 2017).

The cyclic voltammetry (Fig. 9) curves of CuO nanoparticles, recorded at scan rates ranging from 50 - 100 mV/s, exhibit a quasi-rectangular shape, which is indicative of excellent capacitive behavior. The broad redox peaks observed in the CV curves point to faradaic processes that correspond to the reversible redox transitions of Cu^{2+}/Cu^{+}, confirming the pseudocapacitive nature of the material. These pseudocapacitive properties highlight the ability of CuO nanoparticles to store charge not only via electrical double-layer capacitance but also through electrochemical reactions at the electrode surface (Kumar *et al.* 2022).

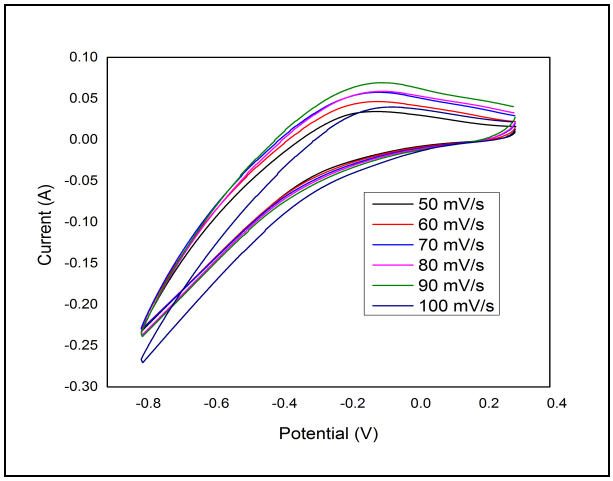


Fig. 9: Cyclic voltammetry (CV) plot of CuO nanoparticles

As the scan rate increases, the area enclosed by the CV curves expands significantly, reflecting the material's capacity to maintain high charge storage performance even at elevated rates. This behavior indicates rapid charge transfer kinetics and a high degree of electrochemical stability. Importantly, the minimal distortion in the shape of the CV curves at higher scan rates underscores the stability of the electrochemical processes occurring within the CuO electrode material.

The combination of excellent capacitive behavior and stability under varying scan rates makes CuO nanoparticles promising candidates for energy storage devices (Ansari *et al*. 2023).

3.8 Electrochemical Impedance Spectroscopy (EIS) Analysis

The Electrochemical Impedance Spectroscopy (EIS) plot of CuO nanoparticles (Fig. 10) provides critical insights into their electrochemical properties.

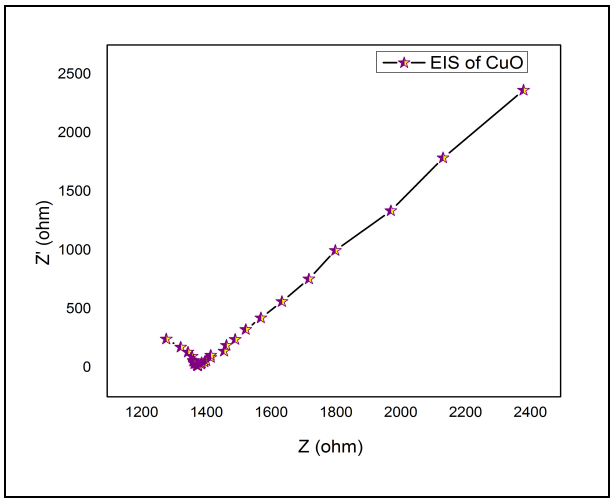


Fig. 10: The electrochemical impedance spectroscopy (EIS) plot for CuO nanoparticles

The linear region in the low-frequency range corresponds to the Warburg impedance, which relates to ion diffusion within the electrode material. The moderate Warburg impedance highlights reasonable ion transport properties, essential for maintaining stable electrochemical performance. Together, the low R_{ct} and moderate Warburg impedance suggest that CuO nanoparticles exhibit superior charge transfer and ion transport properties (Yu *et al.* 2020).

The kinetics of the irreversible reaction can be defin ed using Laviron equation (Jasvinder *et al.* 2021) as,

$$E_p = E^0 + \left(\frac{2.303RT}{\propto nF}\right)\log\left(\frac{RTk^\circ}{\propto nF}\right)\left(\frac{2.303RT}{\propto nF}\right)\log \upsilon \quad \ldots (1)$$

where, E^0 is formal redox potential, α is the transfer coefficient, n-number of electrons transferred, k^0 is the rate constant and ν is scan rate.

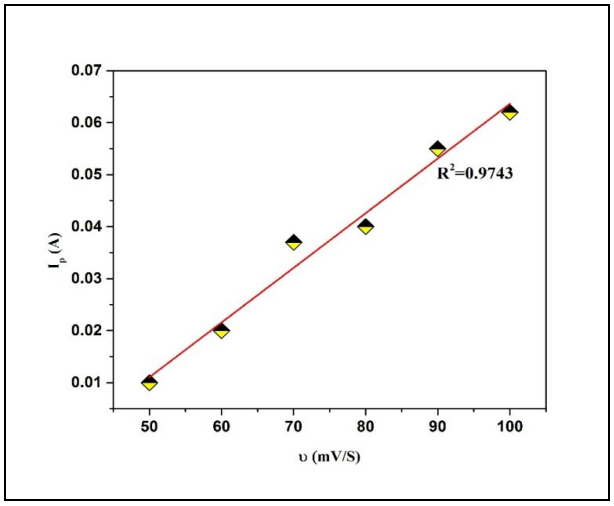


Fig. 11: Plot of peak current vs. scan rate

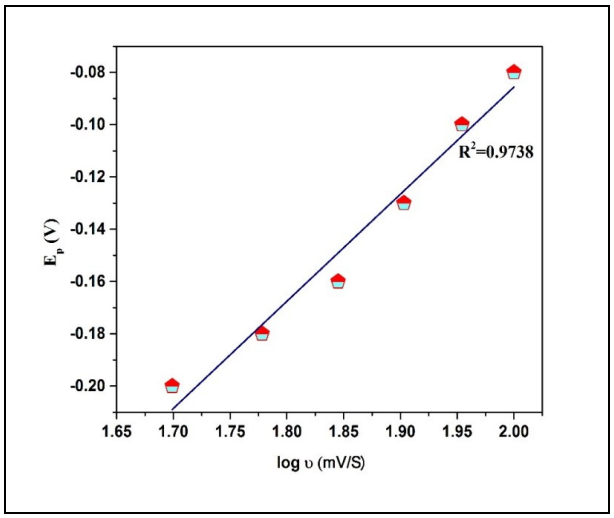


Fig. 12: Laviron plot for CV curves of CuO nanoparticles

The cyclic voltammetry plot reveals an anodic peak, which points to the irreversible nature of the electrochemical process occurring on the electrode surface. This feature is indicative of faradaic reactions associated with the active material's redox behavior. Furthermore, the linear relationship (Fig. 11) observed between the peak current and scan rate confirms that the electrochemical process is adsorption-controlled. The strong linear correlation between peak current and scan rate highlighted the adsorption-controlled nature of the electrochemical reaction. Using the Laviron equation (Fig. 12), the rate constant for the irreversible adsorption-controlled electrochemical process was calculated to be 0.9071×10^{-3} s^{-1}, providing the electrochemical behavior of the system obeys first order kinetics.

4. CONCLUSION

This study provided an in-depth insight about the physicochemical properties of CuO nanoparticles, emphasizing their potential across various applications. The XRD and Raman analyses confirmed the monoclinic phase, high crystallinity, and structural integrity of the CuO nanoparticles. The HRSEM and TEM investigations revealed a porous structure and high surface area, essential for enhancing catalytic and electrochemical efficiency. UV-Vis spectroscopy highlighted a significant quantum confinement effect, with the nanoparticles exhibiting a widened band gap of 3.8 eV, further validating their suitability for optoelectronic and photo catalytic applications.

Electrochemical studies strongly supported the versatility of CuO nanoparticles in energy storage systems. The Nyquist plot demonstrated low charge transfer resistance, reflecting excellent conductivity and stable ion diffusion. Cyclic voltammetry (CV) analysis showed broad redox peaks and a quasi-rectangular profile, confirming pseudo capacitive behavior. The linear correlation between the peak current and the scan rate confirms that the electrochemical process is irreversible and adsorption-controlled. The rate constant for the irreversible electrochemical process was calculated to be $0.9071\times10^{-}3$ s^{-1} using Laviron equation.

FUNDING

There is no funding source.

CONFLICT OF INTEREST

The authors declared no conflict of interest in this manuscript regarding publication.

COPYRIGHT

This article is an open-access article distributed under the terms and conditions of the Creative Commons

Attribution (CC BY) license (http://creativecommons.org/licenses/by/4.0/).



REFERENCES

Ahmed, A. M., Alatawi, A., Hamdalla, T. A., Alfadhli, S. and Darwish, A. A. A., CuO nanoparticles mixed with activated BC extracted from algae as promising material for supercapacitor electrodes, *Sci. Rep.*, 13, 22321(2023). https://doi.org/10.1038/s41598-023-49760-4

Alhalili, Z., Green synthesis of copper oxide nanoparticles CuO NPs from *Eucalyptus Globulus* leaf extract: Adsorption and design of experiments, *Arab. J. Chem.*, 15(5), 103739(2022). https://doi.org/10.1016/j.arabjc.2022.103739

Andualem, W. W., Sabir, F. K., Mohammed, E. T., Belay, H. H. and Gonfa, B. A., Synthesis of copper oxide nanoparticles using plant leaf extract of *catha edulis* and its antibacterial activity, *J. Nanotechnol*, 2020,10(2020). https://doi.org/10.1155/2020/2932434

Ansari, S., Choudhary, R. B. and Gupta, A., Nanoflower copper sulphide intercalated reduced graphene oxide integrated polypyrrole nano matrix as robust symmetric supercapacitor electrode material, *J. Energy Storage.*, 59, 106446 (2023). https://doi.org/10.1016/j.est.2022.106446

Atri, A., Echabaane, M., Bouzidi, A., Harabi, I., Soucase, B. M. and Chaabane, R. B., Green synthesis of copper oxide nanoparticles using *Ephedra alata* plant extract and a study of their antifungal, antibacterial activity and photocatalytic performance under sunlight, *Heliyon.*, 9(2),116(2023). https://doi.org/10.1016/j.heliyon.2023.e13484

Aziz, S.B., Abdullah, O.G. and Rasheed, M.A., Structural and electrical characteristics of PVA:NaTf based solid polymer electrolytes: role of lattice energy of salts on electrical DC conductivity, *J. Mater. Sci: Mater. Electron.*, 28, 12873–12884 (2017). https://doi.org/10.1007/s10854-017-7117-x

Bezza, F. A., Tichapondwa, S. M. and Chirwa, E. M. N., Fabrication of monodispersed copper oxide nanoparticles with potential application as antimicrobial agents, *Sci. Rep.*, 10(1), 16680(2020). https://doi. org/10.1038/s41598-020-73497-z

Crisan, M. C., Teodora, M. and Lucian, M., Copper Nanoparticles: Synthesis and Characterization, Physiology, Toxicity and Antimicrobial Applications, *Appl.Sci.*, 12, 141(2022). https://doi.org/10.3390/app12010141

Grigore, M. E., Biscu, E. R., Holban, A. M., Gestal, M. C. and Grumezescu, A. M., Methods of Synthesis, Properties and Biomedical Applications of CuO Nanoparticles, *Pharm.*, 9(4), 75 (2016). https://doi.org/10.3390/ph9040075

Jasvinder, K., Rajdeep, M. and Dushyant, G., Degradation and evaluation of kinetic parameters of P-Nitrobenzaldehyde: A Cyclic Voltammetry Study, *Ras. J. Chem.*, (Special Issue), 92-97(2021). http://doi.org/10.31788/RJC.2021.1456553

Kamnev, A. A., Dyatlova, Y. A., Kenzhegulov, O. A., Vladimirova, A. A, Mamchenkova, P. V. and Tugarova, A. V., Fourier Transform Infrared (FTIR) Spectroscopic Analyses of Microbiological Samples and Biogenic Selenium Nanoparticles of Microbial Origin: Sample Preparation Effects, *Molecules.*, 26, 1146 (2021). https://doi.org/10.3390/molecules26041146

Kosmaca, J., Katkevics, J., Andzane, J., Sondors, R., Jasulaneca, L., Meija, R., Niherysh, K., Rublova, Y. and Erts, D., Humidity-dependent electrical performance of CuO nanowire networks studied by electrochemical impedance spectroscopy, *Beilstein J. Nanotechnol.*,14, 683-691(2023). https://doi.org/10.3762/bjnano.14.54

Kumar, A., Rathore, H. K., Sarkar, D. and Shukla, A., Nanoarchitectured transition metal oxides and their composites for supercapacitors, *Electrochem. Sci. Adv.*,2(6), 2100187(2022). https://doi.org/10.1002/elsa.202100187

Liu, J., Liu, Z., Pang, Y. and Zhou, H., The interaction between nanoparticles and immune system: application in the treatment of inflammatory diseases, *J. Nano. biotechnol.*, 20, 127-135(2022). https://doi.org/10.1186/s12951-022-01343-7

Mobarak, M. B., Hossain, M. S., Chowdhury. F and Ahmed, S., Synthesis and characterization of CuO nanoparticles utilizing waste fish scale and exploitation of XRD peak profile analysis for approximating the structural parameters, *Arab. J. Chem.*, 15(10), 104117(2022). https://doi.org/10.1016/j.arabjc.2022.104117

Mohamed, A. A., Abu-Elghait, M., Ahmed, N. E. and Salem S. Salem., Eco-friendly Mycogenic Synthesis of ZnO and CuO Nanoparticles for In Vitro Antibacterial, Antibiofilm, and Antifungal Applications, *Biol. Trace Elem. Res.*, 199, 2788–2799(2021). https://doi.org/10.1007/s12011-020-02369-4

Munawar, T., Yasmeen, S., Hussain, F., Mahmood, K., Hussain, A. and Asghar, M., Synthesis of novel heterostructured ZnO-CdO-CuO nanocomposite: Characterization and enhanced sunlight driven photocatalytic activity, *Mater. Chem. Phys.*, 249,122983(2020). https://doi.org/10.1016/j.matchemphys.2020.122983

Pal, B., Mallick, S.S. and Pal, B., Anisotropic CuO Nanostructures of different size and shape exhibit thermal conductivity superior than typical bulk powder, *Colloids and Surfaces A: Physi. Chem. Eng. Asp.*, 459, 282-289(2014). https://doi.org/10.1016/j.colsurfa.2014.07.017

Rehman, S., Mumtaz, A. and Hasanain, S. K., Size effects on the magnetic and optical properties of CuO nanoparticles, *J. Nanopart. Res.*, 13, 2497–2507 (2011). https://doi.org/10.1007/s11051-010-0143-8

Sarfraz, S., Javed, A., Mughal, S.S.,Bashir, M., Rehman, A., Parveen, S., Khushi, A. and Khan, M.K., Copper Oxide Nanoparticles: Reactive Oxygen Species Generation and Biomedical Applications, *Int. J. Comput. Theor. Chem.*, 8, 40–46 (2020). https://doi.org/10.11648/j.ijctc.20200802.12

Tite, T., Chiticaru, E. A. and Burns, J. S., Impact of nano-morphology, lattice defects and conductivity on the performance of graphene based electrochemical biosensors, *J. Nanobiotechnol.*, 17, 101(2019). https://doi.org/10.1186/s12951-019-0535-6

Yu, H. C., Adler, S. B., Barnett, S. A. and Thornton, K., Simulation of the Diffusional Impedance and Application to the Characterization of Electrodes with Complex Microstructures, *Electrochim. Acta.*, 354, 136534(2020). https://doi.org/10.1016/j.electacta.2020.136534